

Submillimeter Pupil-Plane Wavefront Sensing

E. Serabyn and J.K. Wallace
Jet Propulsion Laboratory, 4800 Oak Grove Drive,
California Institute of Technology, Pasadena, CA, 91109, USA

Copyright 2010 Society of Photo-Optical Instrumentation Engineers.

This paper was published in *Millimeter, Submillimeter, and Far-Infrared Detectors and Instrumentation V*, Proc. SPIE 7741, 77410U, and is made available as an electronic reprint with permission of SPIE. One print or electronic copy may be made for personal use only. Systematic or multiple reproduction, distribution to multiple locations via electronic or other means, duplication of any material in this paper for a fee or for commercial purposes, or modification of the content of the paper are prohibited.

Submillimeter Pupil-Plane Wavefront Sensing

E. Serabyn*^a and J.K. Wallace^a

^aJet Propulsion Laboratory, 4800 Oak Grove Drive,
California Institute of Technology, Pasadena, CA, 91109, USA

ABSTRACT

The goal of a large (25 m) submillimeter telescope with high aperture efficiencies up to frequencies of ~ 1 THz requires a wavefront sensor able to measure the telescope surface figure to an accuracy of order 1 micron, better than has been achieved to date in the millimeter/submillimeter (MSM) regime. On the other hand, the recent availability of large-format submillimeter detector arrays suggests that new techniques can be applied. In particular, using submillimeter focal plane arrays, variants of interferometric pupil-plane wavefront sensing techniques familiar from the optical/infrared (OIR) regime could perhaps be applied profitably in the MSM. However, while many possibilities can in principle be considered, many of these possibilities would be unwieldy in the MSM, because of the need for large off-axis reflective optical elements, and the consequent sizeable optical layout. However, the overall size of an interferometer can be minimized by making use of a common-path interferometer. Here we thus consider the applicability to MSM wavefront sensing of a rather simple common-path pupil-plane interferometer, specifically a scanning version of the fixed-phase phase-contrast interferometers described in different contexts by Zernicke¹ and Dicke². Both transmissive and reflective solutions for the needed phase shifting interferometers are possible, but here we focus on the reflective case as a proof of principle. Such a common-path phase-shifting interferometer has several potential advantages: relative simplicity, compactness, ease of manufacturability, reduced systematic effects, and high accuracy.

Keywords: submillimeter, wavefront sensing, holography

1. INTRODUCTION

A MSM telescope as large as 25 m calls for a reliable means of setting the surface accurately. Established MSM surface measurement techniques have not demonstrated the needed micron-level accuracy, but at least one such technique has provided an accuracy of several microns³. However, MSM wavefront sensing techniques used to date have tended to rely on single-pixel detectors, making them inherently slow at mapping, and subject to systematic errors caused by atmospheric and instrumental drifts over the map timescale. On the other hand, the existence of large-format MSM detector arrays suggests that new techniques can now be considered. In particular, pupil-plane wavefront sensing using detector arrays has the potential for greater sensitivity than has been demonstrated in practice to date⁴, and systematics are also minimized because of near-instantaneous measurement of the full pupil. Moreover, it may be possible to translate a wavefront sensing technique already established in the OIR, where detector arrays are ubiquitous.

The MSM and OIR regions differ significantly in several regards. First, seeing variations are much slower in the MSM than in the OIR. Thus instead of wavefront sensing at kHz rates, MSM timescales are set instead by the timescales over which the MSM diffraction point spread function (PSF) changes significantly due to e.g. gravitational or thermal deformation of the telescope, or to atmospheric transmission changes caused by variations in the water vapor column overhead. On the other hand, the signal-to-noise (SNR) related issues all tend to be worse in the MSM, including the atmospheric transmission, the thermal background, and the photon noise aspects, especially as the photon noise at long-wavelengths must include photon bunching⁴. Finally, the linear size of the focal plane PSF in the MSM is much larger than in the OIR. Specifically, for a focal ratio, F , of 8, and a wavelength, λ , in the range 0.3 to 1.0 mm, the full-width at half maximum (FWHM) of the PSF, given roughly by the product $F\lambda$, is about 2.4 to 8 mm across. Since wavefront sensing requires collecting the information contained in a diffraction pattern many $F\lambda$ across ($\sim 30 - 100$), sizable optics are thus called for in the wavefront sensing beamtrain, unless only the shortest wavelengths (~ 0.35 mm) are used.

*gene.serabyn@jpl.nasa.gov; phone 1 818 393-5243; fax 1 818 393-5243

2. INTERFEROMETRIC WAVEFRONT SENSORS

The ultimate sensitivity of interferometric pupil plane wavefront sensors in the MSM has been addressed in a previous paper⁴, wherein a large potential gain in sensitivity and speed over earlier techniques was predicted. However, the optical solutions considered therein were merely illustrative concepts, and were not optimal. In this paper, we thus instead focus on describing a specific interferometric solution appropriate to the MSM case.

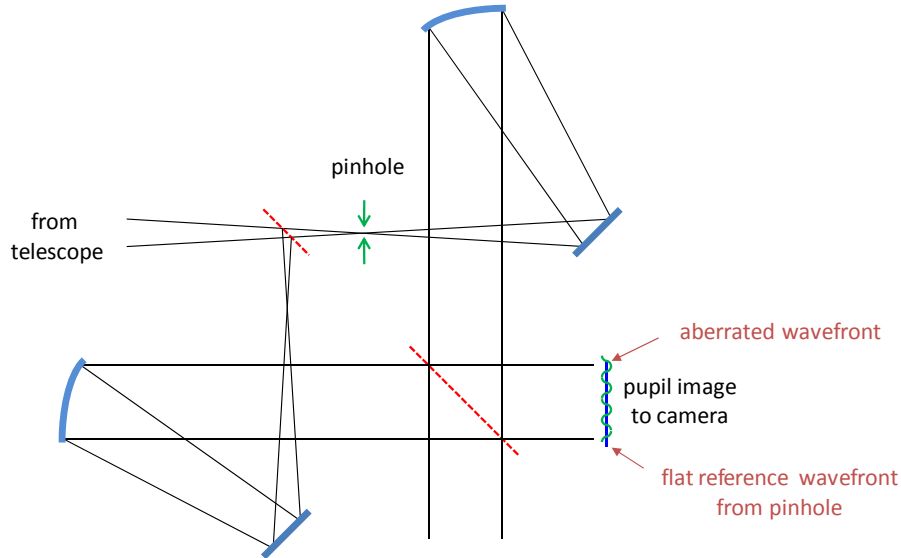


Figure 1. Layout of an all-reflective dual-beam point diffraction interferometer. Because of the physical size of the diffraction pattern, the individual optics would need to be ~ 30 cm across, leading to a sizeable layout.

To begin, we note that any interferometric wavefront sensor requires some means of generating a relatively error-free reference beam, and then of combining the reference beam with the test beam containing the wavefront errors to be measured. However, two-beam MSM wavefront-sensing interferometers can grow quite large and unwieldy as a result of the large linear scale of the PSF in the MSM, and the need for a pair of beamsplitters in the optical train. For example, the case of a point-diffraction interferometer, in which the light in one arm of the interferometer passes through a small pinhole in order to generate a clean reference beam, is shown in Fig. 1, where it can be seen that a number of large optical elements spread out over an area ~ 1 m across would be required to generate the desired pupil plane interference.

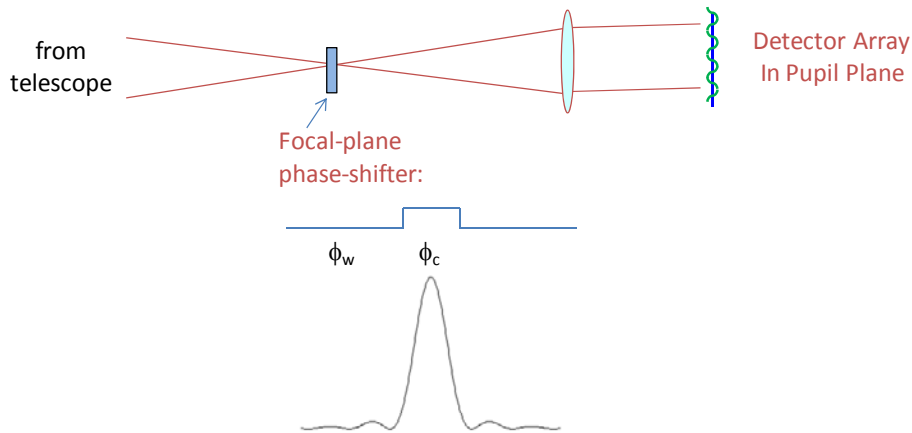


Figure 2. Layout of a transmissive phase-contrast interferometer.

On the other hand, common-path interferometers, in which the reference and test beams traverse the same optics, are also possible, with much more compact layouts. In particular, related to the point diffraction interferometer is the general class of “phase-contrast” interferometers^{1,2}, in which the small pinhole passing the center of the PSF is replaced by a small central disk-like region in which a phase offset relative to the rest of the PSF is applied. Note in particular that such common-path interferometers have no need for beamsplitters, and that the transmissive version of such an interferometer² has a very simple layout (Fig. 2).

However, the main problem with such an approach is that a single phase shift is insufficient to determine the desired pupil plane phase distribution unambiguously. Thus, what is needed is a scanning phase-contrast interferometer, wherein the phase shift that is applied to the core of the PSF is scanned or stepped over a wavelength in phase relative to the remainder of the PSF. In the OIR, this has been difficult to achieve in practice until recently, but solutions have emerged in the last decade⁵⁻⁸. However, the MSM has a distinct advantage in this regard, because the large linear size of the diffraction core ($F\lambda \sim$ a few mm) makes it possible to consider using a small scanning mirror as the phase shifter⁸. Thus, to shift the core of the PSF relative to the rest of the PSF at MSM wavelengths, one can envision installing a small (few mm diameter) scanning mirror at the center of a larger fixed mirror, as in Fig. 3. This can be done at Cassegrain focus (Fig. 3), or in a downstream cat’s eye configuration (Fig. 4).

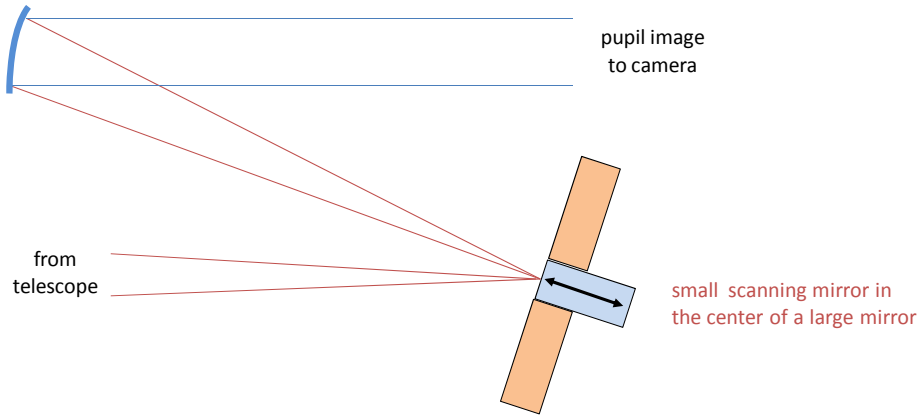


Figure 3. Layout of a reflective scanning phase-contrast interferometer. If desired, the phase shifting mirror assembly could be installed directly at the Cassegrain focus.

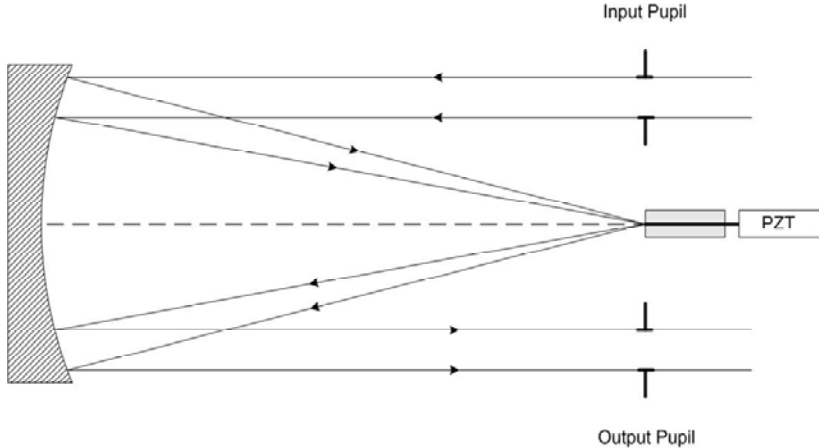


Figure 4. Cat’s eye configuration for a downstream scanning phase-contrast interferometer.

3. OPERATION OF A SCANNING PHASE-CONTRAST INTERFEROMETER

The first question to address is how small the central phase shifting region needs to be. The goal is to provide a relatively uniform reference field across the aperture, so it must be relatively small. As Figure 5 shows, a pinhole diameter of order $F\lambda$ is needed.

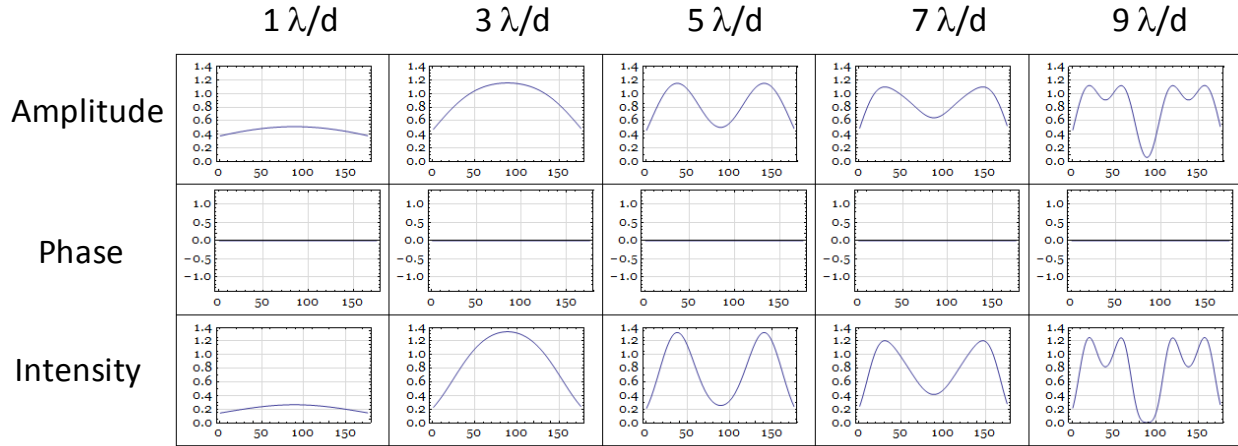


Figure 5. Pupil plane amplitude, phase and intensity vs. focal-plane mask diameter.

In the pupil plane following the “mask” plane, the field will then be a combination of the reference field and the true pupil plane field. After expanding the $e^{i\phi}$ pupil phase error term (in the absence of amplitude errors) this yields

$$E_{\text{pup}} = R + iA\phi,$$

where R is the reference field and A describes the amplitude of the error term. Upon squaring the field, the cross term then produces an intensity term linearly proportional to the desired phase error. Measurements of the resultant pupil plane intensity thus yield the distribution of pupil phase errors.

3.1 Example

The operation of such a phase-contrast interferometer is illustrated in Figures 6, 7 and 8. A test phase-error pattern consisting of the superposition of two sine-wave phase-error components is assumed. Fig. 6 shows the input field, Fig. 7 shows the pupil plane intensity distribution for four quadrature phase settings, and Figure 8 shows the recovered phase distribution. As Fig. 8 illustrates, with this approach, pupil-plane phase errors can be recovered with high fidelity.

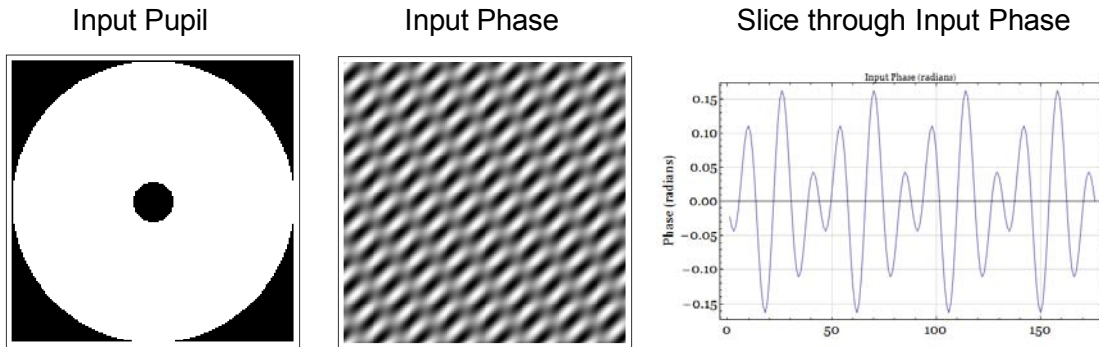


Figure 6. Model input field with a uniform amplitude and two sine-wave phase-error terms.

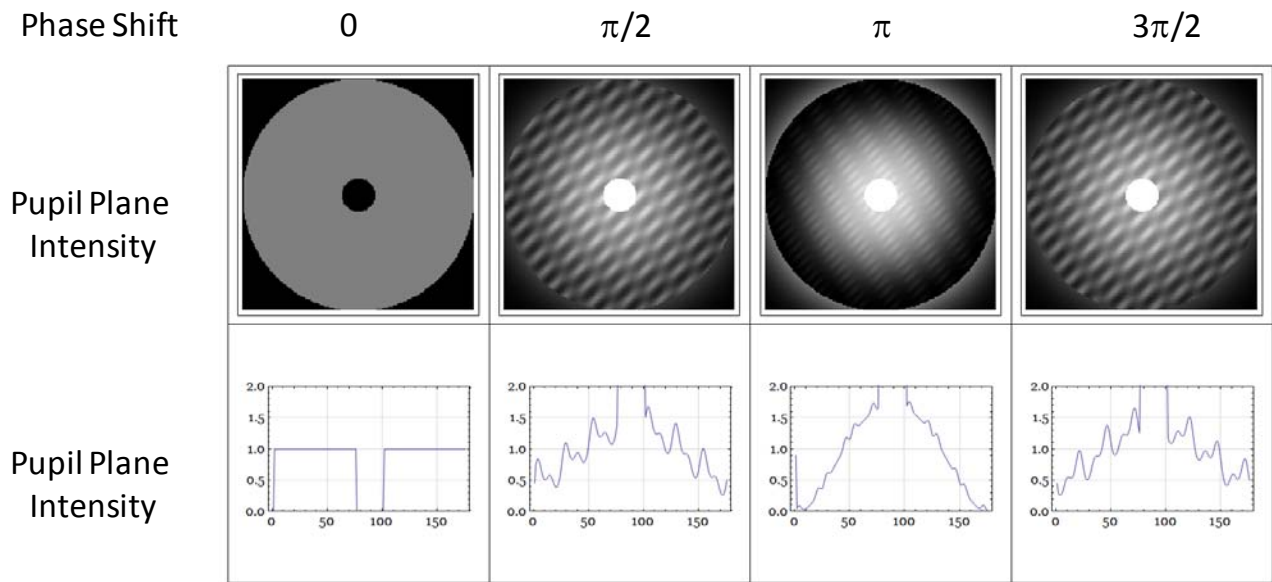
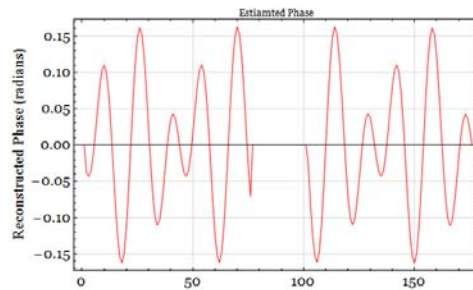
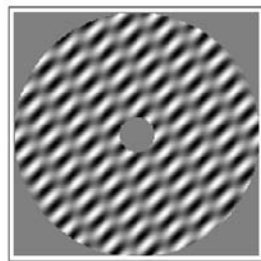


Figure 7. Resultant interferometer output pupil-plane intensity distribution for the two sine-wave error input, for four quadrature values of the phase shift. Note that the phase errors are obvious at phase shifts at $\pi/2$ and $3\pi/2$.

Phase Estimate



Comparison of Input and Estimated Phase

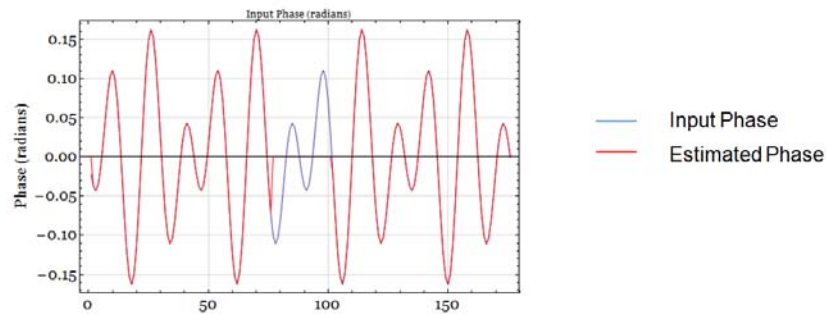


Figure 8. Results of the measurement. The phase measurement is obtained essentially by differencing the pupil intensities obtained at $\pi/2$ and $3\pi/2$. In the presence of amplitude errors, all four quadrature terms are required.

4. CONCLUSIONS

A common-mode phase-shifting interferometer should be capable of high-fidelity pupil-plane wavefront sensing in the MSM region, and should also be relatively straightforward to construct. Such a common-path phase-shifting interferometer has several potential advantages, including relative simplicity, compactness, ease of manufacturability, reduced systematic effects, and high accuracy. More detailed modeling is now needed, and a laboratory or on-sky demonstration would be an obvious next step.

The research described herein was carried out at the Jet Propulsion Laboratory, California Institute of Technology, under contract with NASA.

REFERENCES

- [1] Zernicke, F., *Z. Tech. Phys.* 16, 454 (1935).
- [2] Dicke, R.H., *Astrophys. J.* 198, 605 (1975).
- [3] Serabyn, E., Phillips, T.G. & Masson, C.R., *Applied Optics* 30, 1227 (1991).
- [4] Serabyn, E., *Proc. SPIE* 6275, 62750Z-1 (2006).
- [5] Mercer, C.R. & Creath, K., *Applied Optics* 35, 1633 (1996).
- [6] Vorontsov, M.A., Justh, E.W. & Beresnev, L.A., *J. Opt. Soc. Am. A* 18, 1289 (2001).
- [7] Millerd, J.E., Brock, N.J., Hayes, J.B. & Wyant, J.C., *Proc. SPIE* 5531, 264 (2004).
- [8] Wallace, J.K., in prep.